Atmospheric Research 202 (2018) 33–39

Contents lists available at ScienceDirect

Atmospheric Research

journal homepage: www.elsevier.com/locate/atmosres

Impact of primary and secondary air supply intensity in stove on emissions of size-segregated particulate matter and carbonaceous aerosols from apple tree wood burning

Jian Sun[a,b], Zhenxing Shen[a,b,*], Leiming Zhang[c], Qian Zhang[a], Yali Lei[a], Junji Cao[b], Yu Huang[b], Suixin Liu[b], Chunli Zheng[a], Hongmei Xu[a], Hongxia Liu[a], Hua Pan[a], Pingping Liu[a], Renjian Zhang[d]

[a] Department of Environmental Sciences and Engineering, Xi'an Jiaotong University, Xi'an 710049, China
[b] Key Lab of Aerosol Chemistry & Physics, SKLLQG, Institute of Earth Environment, Chinese Academy of Sciences, Xi'an 710049, China
[c] Air Quality Research Division, Science and Technology Branch, Environment and Climate Change Canada, Toronto, Canada
[d] Key Laboratory of Regional Climate-Environment for Temperate East Asia, Institute of Atmospheric Physics, Chinese Academy of Sciences, Beijing 100029, China

ARTICLE INFO

Keywords:
Emission factors
Carbonaceous aerosol
Secondary air supply
Semi-gasifier stove
Wood burning

ABSTRACT

In order to assess emission factors (EF) more accurately from household biomass burning, a series of laboratory-controlled apple tree wood burning tests were conducted to measure the EFs of size-segregated particulate matter (PM) and carbonaceous aerosols. The controlled burning experiments were conducted with designed primary air (PA) and secondary air (SA) supply intensity. An optimum value of 7 $m^3 \cdot h^{-1}$ was found for SA, resulting the highest modified combustion efficiency (92.4 ± 2.5%) as well as the lowest EFs of $PM_{2.5}$ (0.13 ± 0.01 $g \cdot MJ^{-1}$), OC (0.04 ± 0.03 $g \cdot MJ^{-1}$) and EC (0.03 ± 0.01 $g \cdot MJ^{-1}$). SA values of 7 and 10 $m^3 \cdot h^{-1}$ resulted the lowest EFs for all the different PM sizes. In a test with PA of 6 $m^3 \cdot h^{-1}$ and SA of 7 $m^3 \cdot h^{-1}$, very low EFs were observed for OC1 (8.2%), OC2 (11.2%) and especially OP (Pyrolyzed OC) (0%, not detected), indicating nearly complete combustion under this air supply condition. Besides SA, higher PA was proved to have positive effects on PM and carbonaceous fraction emission reduction. For example, with a fixed SA of 1.5 $m^3 \cdot h^{-1}$, EFs of $PM_{2.5}$ decreased from 0.64 to 0.27 $g \cdot MJ^{-1}$ when PA increased from 6 to 15 $m^3 \cdot h^{-1}$ ($P < 0.05$). Similar reductions were also observed in EFs of OC, EC and size segregated PM.

1. Introduction

For the last three decades, about 2.8 billion persons relied on solid fuels (biomass such as wood, crop residues, dung and charcoal) for cooking and heating globally, and this was still the case in 41% of total households in 2010 (Bonjour et al., 2013; Kirch et al., 2016). Solid fuel burning emits large quantities of pollutants into atmosphere (Shen et al., 2009; Kjallstrand and Olsson, 2004; Xu et al., 2016), such as $PM_{2.5}$ (particulate matters with aerodynamic diameter < 2.5 μm), organic carbon (OC), elemental carbon (EC), polycyclic aromatic hydrocarbons (PAHs), etc. Residential solid fuel burning was the largest contributor to OC and $PM_{2.5}$ emissions (Lei et al., 2011), the second largest to PAHs emissions (Xu et al., 2006), and the third largest to BC emissions (Wang et al., 2012). Household air pollution from solid fuels was a major cause of diseases in women and children globally and is responsible for 50% of premature deaths under five years of age (WHO, 2014).

Residential wood combustion is of wide concern in China due to its adverse impacts on air quality and human health, especially in some mountainous areas and fruit production regions (Shen et al., 2012). For example, in Guanzhong Plain of Northwest China, apple trees are commonly planted as the main commercial crops. Branches of these trees are produced from clipping activities every winter and are mainly used as fuels by local residents for cooking and heating. To make things worse, most wood stoves used for residential heating today are still old-fashioned and emit large quantities of pollutants (Kjallstrand and Olsson, 2004). Thus, a great effort has been made from government agencies and scientific communities to reduce residential stove emissions. For example, the Chinese government implemented the National Improved Stove Program (NISP) from 1982 to 1992 by replacing traditional stoves by high thermal-efficient ones, and has effectively reduced indoor air pollution (Chowdhury et al., 2013). Earlier studies have observed that using two-stage stoves especially those with forced air increased heat transfer efficiency and decreased emitted pollutants from incomplete combustion, foremost CO and PM, compared to the old-fashioned stoves (MacCarty et al., 2010; Kumar et al., 2013; Raman

* Corresponding author at: Department of Environmental Sciences and Engineering, Xi'an Jiaotong University, Xi'an 710049, China.
E-mail address: zxshen@mail.xjtu.edu.cn (Z. Shen).

https://doi.org/10.1016/j.atmosres.2017.11.010
Received 15 April 2017; Received in revised form 7 October 2017; Accepted 6 November 2017
Available online 09 November 2017
0169-8095/

et al., 2014). However, not every newly designed stove improved the emission control despite with more energy efficient (Kshirsagar and Kalamkar, 2014), e.g. some stoves with increased release of ultra-fine particles (particulate matters with aerodynamic diameter < 1.0 μm) (Jetter et al., 2012).

Sufficient air supply and complete mixing between air and fuel were key factors for complete combustion (Shen et al., 2012; Kirch et al., 2016). In recent years, many two-stage wood stoves with forced or natural secondary air supply system entered the market. Emission factors of pollutants from the newly designed wood stoves varied substantially and systematic investigations were needed to understand the influence of air supply to wood stove emissions (Wiinikka and Gebart, 2005; Shen et al., 2012). In addition, it is widely reported in previous studies that the uncertainties in results from field experiments were extremely high (even over 200%) (Such as Tian et al., 2015). The present study is thus designed to investigate EFs of size segregated particles and carbonaceous species from a two-stage wood stove under various air supply and distribution conditions. Knowledge gained from the study will be useful in designing new stoves and accurately quantifying pollutants emissions from household biomass burning.

2. Materials and methodology

2.1. Research stove

A two-stage solid fuel stove (Fig. S1) was designed to provide controlled air flow rates in both primary air (PA) and secondary air (SA). PA is controlled by varying the window of PA inlet while SA is controlled by a blower with a power of 5 W installed at the SA inlet. In this stove, PA is connected to the gasifier chamber supplying air (oxygen) for gasification reactions which produces combustible mixture including gases (CO, CH_4, C_2H_6 and etc.) and particles. SA is connected to the combustion chamber providing air mixing directly with combustible mixture. A heat exchanger is set at the starting point of the flue chimney and collected with a 20 L-water tank. The tank is commonly connected to an indoor heating system to provide heating, but in this study, indoor heating system was not connected and all water used in test was stored in the tank for measuring weight loss and temperature rise which could reflect the heating transfer efficiency of the stove.

2.2. Fuel

Apple trees wood chips from a garden clip waste in Guanzhong Plain, China were used as fuels for the tests reported in this study. Wood chips were cut into pellets with a size varying from 30 (L) × 30 (D) mm to 50 (L) × 50 (D) mm in approximately cylinder shape to ensure a steady and controllable experimental condition. A controlled moisture content and industrial analysis was done before the experiments and the results are shown in Table S1a and Table S1b. The mass of fuel for each test was ~2.0 kg.

2.3. Measurements

A combustion chamber was set up in a laboratory at the Institute of Earth Environment, Chinese Academy of Sciences (IEECAS) to simulate the burning of biomass. The combustion chamber was equipped with a thermocouple, a thermo anemometer, an air purification system, and a sampling line connected to a dilution sampler (Wang et al., 2009). Samples of the combustion emissions were collected using a custom-made dilution system with dilution ratios ranging from 5- to 15-fold. The details of this dilution system were described in Tian et al. (2015). Dilution samplers were connected with three parallel channels located downstream of the residence chamber, and $PM_{2.5}$ samples were collected on quartz membrane with a flow rate of 5 $L{\cdot}min^{-1}$. Size segregated PM samples were collected using an eight-stage cascade impactor sampler (Anderson, Thermo Fisher Scientific, Franklin, MA, USA) with 80 mm diameter quartz membranes at a flow rate of 28.3 $L{\cdot}min^{-1}$. Real-time CO levels were monitored by a CO analyzer (Model 48i, Thermo Scientific Inc., Franklin, MA, USA) (Wang et al., 2009). Three non-dispersive infrared (NDIR) CO_2 analyzers (Model SBA-4, PP Systems, Amesbury, MA, USA) were used to measure CO_2 levels on background, in the stack, and in diluted emissions, respectively. And for each condition, duplication tests were conducted at least 3 times to avoid experimental errors and accidental errors.

All filter samples collected in this study were kept at − 20 °C before being analyzed. First of all, gravimetric analysis of particle mass loadings was determined by a Sartorius MC5 electronic microbalance (± 1 μg sensitivity, Sartorius, Gottingen, Germany). OC and EC in PM samples were analyzed using a Thermal and Optical Carbon Analyzer (Model 2001, AtmAA Inc., USA) with IMPROVE (Interagency Monitoring of Protected Visual Environment) thermal/optical reflectance (TOR) protocol. Detailed operation procedures were described in Sun et al. (2017).

2.4. Data analysis methods

EFs of particulate and gaseous pollutants were calculated based on heat transferred with unit of g· or $mg{\cdot}MJ^{-1}$, with input parameters including the diluted concentration of a pollutant (C_{Dil}), the dilution ratio (DR), sampling duration (t_{sample}), fuel consumption (m_{fuel}), sampling volume (Q_{filter}), stack flow velocity (V_{Stk}), low heating value (LHV) of fuel, thermal efficiency (TE), and stack cross section area (D), as detailed in Sun et al. (2017).

For particulate pollutants (i.e. $PM_{2.5}$, OC and EC), the EF_p is:

$$EF_p = \frac{m_{filter} \times DR \times t_{sample} \times V_{stk} \times D}{Q_{filter} \times m_{fuel} \times LHV \times TE} \quad (1)$$

Modified combustion efficiency (MCE) was calculated based on measured CO and CO_2. It is widely reported to differentiate flaming and smoldering phase in combustion (McMeeking et al., 2009; Ni et al., 2015). The formula is as below:

$$MCE = \Delta[CO2]/(\Delta[CO2] + \Delta[CO]) \quad (2)$$

where Δ[CO2] and Δ[CO] are the excess molar mixing ratios of CO_2 and CO, respectively.

3. Results & discussion

3.1. Implication of air supply on MCE

Table 1 shows the descriptions and parameters of each independent test in this study. Besides flow rates of PA and SA, oxygen concentrations in exhaust smoke were also measured. A proper excess air ratio, which could be calculated by O_2 concentration in smoke, is widely accepted to be necessary for high efficient combustion and low pollutants emission (Ryu et al., 2006; Xie et al., 2007). The high excess air ratios suggested that the system operated at fuel-lean conditions with all PA and SA flow rates.

MCE was calculated for each test to offer a quantized parameter in distinguishing flaming and smoldering during combustion process. Thermal efficiency and heating rates were used to evaluate the capability of thermal transfer in different stoves and working conditions and were extracted from water boiling test (WBT) (Bailis et al., 2007). In Table 1, Tests 1–6 were designed to detect the impact of secondary air supply on PM and carbonaceous particle emissions, and thus had the same PA flow (6 $m^3{\cdot}h^{-1}$) but varying SA flow from 0.3 to 15 $m^3{\cdot}h^{-1}$. In this SA range, an optimum value of 7 $m^3{\cdot}h^{-1}$ was found which produced the highest MCE value (92.4 ± 2.5%, $P < 0.05$) and also the best performance in terms of thermal efficiency and heating rate (Fig.1).With SA being set as 7 $m^3{\cdot}h^{-1}$, MCE kept at high levels for a relatively long time period. In contrast, with SA being set as 0.3 $m^3{\cdot}h^{-1}$, the MCE curve was the lowest among all the test series and the

Table 1
Description, air distribution and coefficient of excess air of different tests.

Test no.	PA, m^3/h	SA, m^3/h	PA/SA	O_2 in smoke, %	coefficient of excess air	Heating rate, °C/min	Thermal efficiency, %	MCE, %
1	6.0	0.3	20.0	8.6	1.7	2.4	33.6	74.4 ± 1.5
2	6.0	1.5	4.0	8.9	1.7	3.0	39.0	80.2 ± 0.1
3	6.0	4.0	1.5	9.5	1.8	3.6	47.8	85.4 ± 6.1
4	6.0	7.0	0.9	12.4	2.5	4.4	68.0	92.4 ± 2.5
5	6.0	10.0	0.6	13.7	2.9	3.9	58.9	85.3 ± 8.1
6	6.0	15.0	0.4	14.9	3.5	3.8	56.7	79.6 ± 3.1
7	15.0	1.5	10.0	9.8	1.9	4.1	60.6	89.9 ± 2.0
8	15.0	15.0	1.0	15.8	4.1	4.5	70.8	91.2 ± 1.9

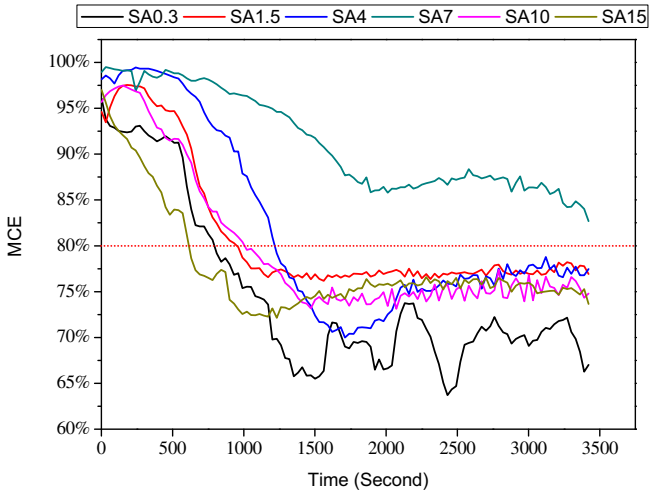

Fig. 1. Time series of MCE in same PA (6 $m^3 \cdot h^{-1}$) but different SA conditions.

combustion status was mostly unstable as well. Thus, with increasing SA up to the optimum value of 7 $m^3 \cdot h^{-1}$, more air was introduced to downstream reaching to the front flame, enabling more complete mixing of air with the primary combustion products and resulting more complete combustion and then higher MCE and TE (Kirch et al., 2016). However, further increasing SA provided excess air diluting the heat in combustion chamber and decreasing temperature, which in turn leading more CO emission (lower MCE) and lower thermal transfer efficiency (Johansson et al., 2003; Houshfar et al., 2011). An earlier study suggested the optimized excess air ratio to be around 2.0 (Liu et al., 2001), while the present study found it to be 2.5 for best performance (Test 4).

Fig. 2 shows the time series of MCE under two different PA flows with fixed SA conditions of 1.5 and 15 $m^3 \cdot h^{-1}$. It was seen that higher PA enhanced the MCE level when SA was fixed. For example, Test 7 (89.9% ± 2.0%) had higher MCE than Test 2 (80.2% ± 0.1%) and Test 8 (91.2% ± 1.9%) higher than Test 6 (79.6% ± 3.1%) ($P < 0.05$), so was the case for TE and heating rate ($P < 0.05$) (Table 2). PA was proved to control the combustion rate of solid fuel, and thus residential users shut down PA inlet when keeping a long combustion period (Sun et al., 2017). As mentioned above, all the tests were in oxygen rich condition, and thus fast fuel burning rates led by higher PAs should transfer more heat in a unit time, which had been observed in this study. The highest heating rate measured in Test 8 was 4.5 °C·min^{-1} (for 6 kg water in WBT), which was obviously higher than that in Test 6 (3.8 °C·min^{-1}). A similar contrast was also observed between Tests 2 and 7.

3.2. Implication of air supply on EFs of PM

$PM_{2.5}$ was deemed as the most serious pollutant emitted from solid fuel combustion especially in residential use (Shen et al., 2010; Sun et al., 2017). A lot of parameters including stove type, fuel type, air supply, etc. have been proved to impact $PM_{2.5}$ emission in solid fuel combustion (Chen et al., 2012; Jetter et al., 2012). Table 2 lists heat transfer based $PM_{2.5}$ emission factors under different SA conditions. With a fixed PA (6 $m^3 \cdot h^{-1}$), SA shows a non-linear influence on EFs of $PM_{2.5}$ ($EF_{PM2.5}$). The lowest $EF_{PM2.5}$ (0.13 ± 0.01 g·MJ^{-1}) was observed in Test 4 with SA being 7 $m^3 \cdot h^{-1}$. This extremely low EF was likely due to the optimal secondary air supply combined with proper PA, as supported by the excess air ratio of 2.5 found in this test, which is close to the literature reported optimized value of 2.0 mentioned above. $EF_{PM2.5}$ increased when SA diverted from the optimum value of 7 $m^3 \cdot h^{-1}$. Lower SA than this value could not provide sufficient secondary air supply for complete combustion (leading to the highest EFs at 0.3 $m^3 \cdot h^{-1}$) and higher SA than this value cool down the combustion chamber due to too much excessed air which may also lead to incomplete combustion (Shen et al., 2010). This hypothesis was

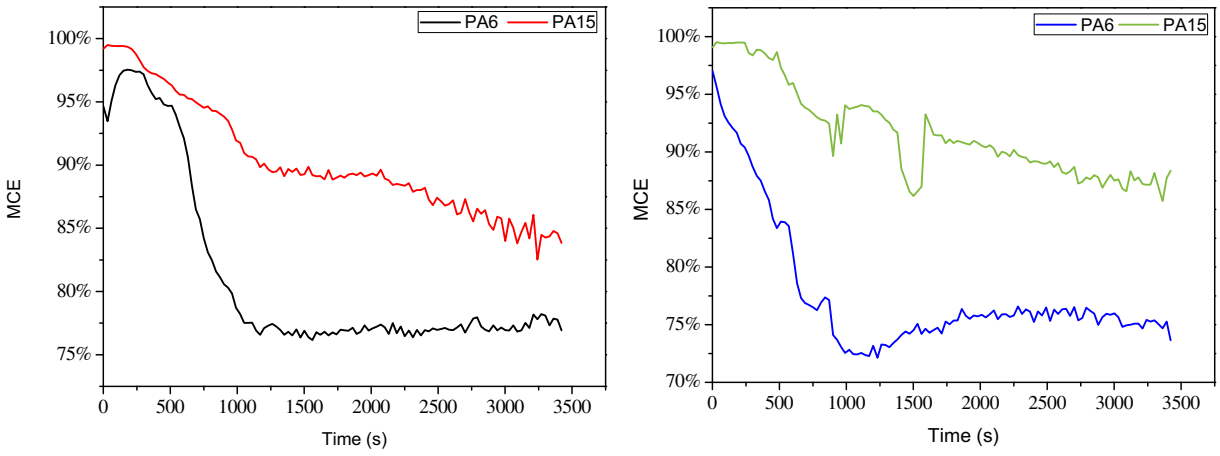

Fig. 2. Time series of MCE in same SA (1.5 $m^3 \cdot h^{-1}$ for left and 15 $m^3 \cdot h^{-1}$ for right) but different PA conditions.

Table 2
EFs of $PM_{2.5}$ and carbonaceous fraction in $PM_{2.5}$ in varied SA tests.

Test no.	$EF_{PM2.5}$, g·MJ^{-1}	EF_{TC}, g·MJ^{-1}	EF_{OC}, g·MJ^{-1}	EF_{EC}, g·MJ^{-1}	OC/EC ratio
1	1.77 ± 0.26	0.94 ± 0.07	0.80 ± 0.61	0.14 ± 0.13	5.9
2	0.64 ± 0.06	0.39 ± 0.07	0.24 ± 0.23	0.14 ± 0.01	1.7
3	0.27 ± 0.04	0.12 ± 0.03	0.08 ± 0.07	0.05 ± 0.01	1.6
4	0.13 ± 0.01	0.07 ± 0.03	0.04 ± 0.03	0.03 ± 0.01	1.4
5	0.35 ± 0.02	0.18 ± 0.02	0.11 ± 0.12	0.08 ± 0.01	1.5
6	0.42 ± 0.01	0.23 ± 0.02	0.16 ± 0.15	0.07 ± 0.00	2.2

Table 3
EFs of $PM_{2.5}$ and carbonaceous fraction in $PM_{2.5}$ in varied PA tests.

Test no.	$EF_{PM2.5}$, g·MJ^{-1}	EF_{TC}, g·MJ^{-1}	EF_{OC}, g·MJ^{-1}	EF_{EC}, g·MJ^{-1}	OC/EC ratio
2	0.64 ± 0.06	0.39 ± 0.07	0.24 ± 0.23	0.14 ± 0.01	1.7
7	0.27 ± 0.01	0.14 ± 0.00	0.08 ± 0.10	0.06 ± 0.01	1.4
6	0.42 ± 0.01	0.23 ± 0.02	0.16 ± 0.15	0.07 ± 0.00	2.2
8	0.25 ± 0.02	0.17 ± 0.00	0.11 ± 0.12	0.06 ± 0.00	2.0

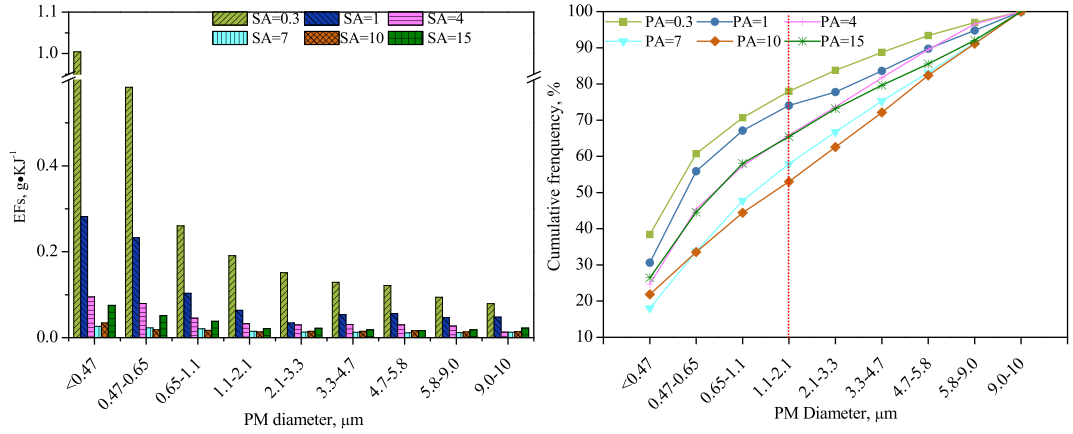

Fig. 3. PM size distribution in same PA (6 m^3·h^{-1}) but different SA conditions.

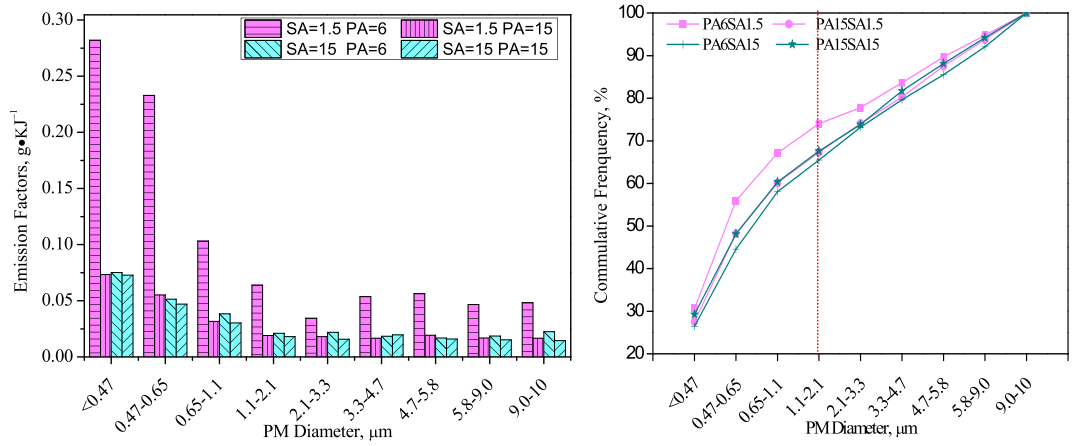

Fig. 4. PM size distribution in same SA but different PA conditions.

supported by the finding that Test 6 had higher EFs of OC (EF_{OC}) (0.16 ± 0.15 g·MJ^{-1}) but lower of EC proportion (0.30, calculated as 0.07/(0.07 + 0.16)) than Test 5 (0.11 ± 0.12 g·MJ^{-1} and 0.42, calculated as 0.08/(0.08 + 0.11)) ($P < 0.05$), knowing that higher OC emission was an indicator of incomplete combustion while higher EC proportion for more complete combustion and higher combustion temperature in certain air supply conditions (Han et al., 2010). The markedly decreases in EF_{OC} and increase in EC proportion when SA moved to the optimum value also resulted in the lowest OC/EC ratio (1.4) in Test 4.

Besides SA, PA also has crucial influence on $PM_{2.5}$ emissions from stove wood burning. It can be seen from $EF_{PM2.5}$, OC and EC from two sets of PA tests (Table 3). Lower EFs were observed in higher PA flow ($P < 0.05$), i.e. Test 7 versus Test 2 and Test 8 versus Test 6. Under the higher SA condition in combustion chamber (15 m^3·h^{-1} in Tests 6 and 8), higher PA matches the higher SA producing more combustible gases and particles in gasification chamber and resulting in high MCE and low EFs. However, it was hard to explain the lower SA condition

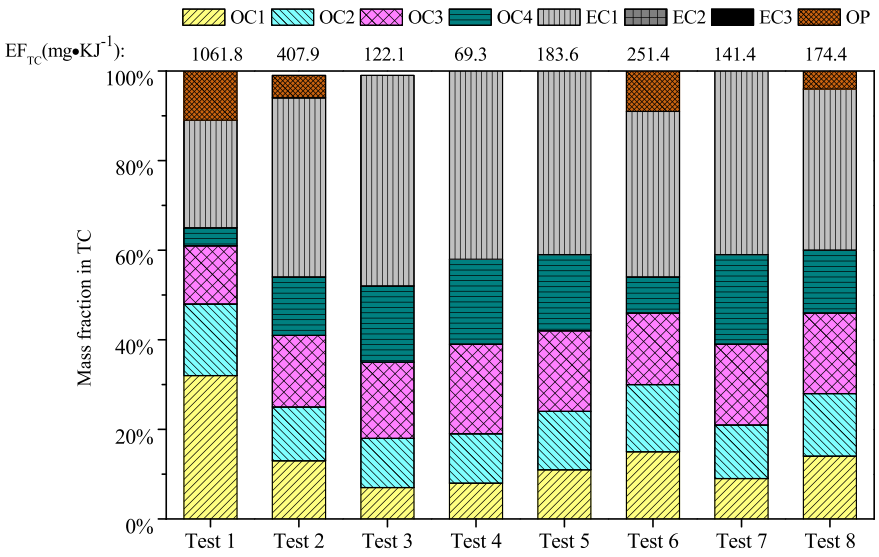

Fig. 5. Mass percentage of thermally resolved organic carbon (OC) and elemental carbon (EC) fractions in $PM_{2.5}$ following IMPROVE_A protocol (Chow et al., 2007). OC1 to OC4 evolve in a 100% helium atmosphere, EC1 to EC3 evolve in a 98% helium/2% oxygen atmosphere. Pyrolyzed OC is the difference between OC and (OC1 + OC2 + OC3 + OC4), and the EC1 values are corrected here by subtracting OP from the original EC1 value.

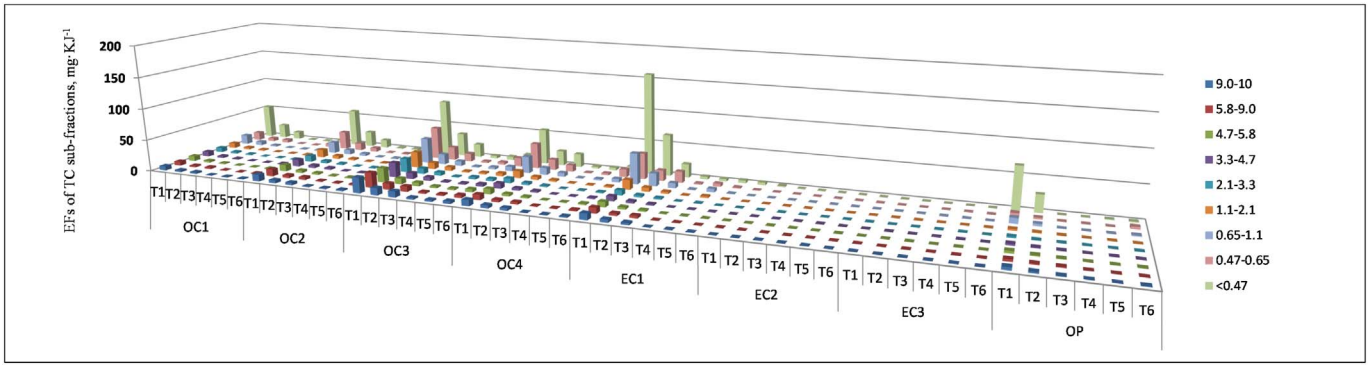

Fig. 6. EFs of TC sub-fractions in tests with consistent PA but varied SA conditions. (PA = 6,varied SA for T1 = 0.3,T2 = 1.5, T3 = 4, T4 = 7, T5 = 10, T6 = 15 m^3/h).

(1.5 $m^3 \cdot h^{-1}$) (Tests 2 and 7) when higher PA (Test 7) still resulted in higher MCE and lower EFs. It could be due to the excess air ratio which showed a slightly higher value in Test 7 than Test 2 (1.88 versus 1.78) and both tests were in oxygen-enriched environment. SA flow could offer more oxygen in Test 7 than Test 2.

Size distributions of PM emitted from wood burning under different SA flows were compared in Fig. 3. EFs of PM (EF_{PM}) in 9 sizes were the lowest at SA values of 7 and 10 $m^3 \cdot h^{-1}$ in all the nine size stages. The highest EFs of size segregated PM were observed in Test 1 with SA being 0.3 $m^3 \cdot h^{-1}$. This could be partly explained by the oxygen deficient condition in the second combustion chamber which produced high emissions from incomplete combustion (Simoneit, 2002; Shen et al., 2013). When SA was larger than 10 $m^3 \cdot h^{-1}$, the EFs of PM in all size stages were higher than those from SA of 7 $m^3 \cdot h^{-1}$. The cumulative frequencies followed the same trends as EF_{PM}. The sum of the first four size stages ($PM_{2.1}$) accounted for 78.0%, 74.0%, 65.5%, 57.8%, 53.0% and 65.5% of the total PM measured in the six SA tests, respectively. And the ultrafine stages ($PM_{1.1}$) also showed a nadir in SA of 10 $m^3 \cdot h^{-1}$. The non-liner impacts of secondary air supply were also observed in previous studies, especially on PM size distribution (Hedberg et al., 2002; Shen et al., 2013).

The impact of PA on EF_{PM} and PM size distribution is shown in Fig. 4. When SA was set as 1.5 $m^3 \cdot h^{-1}$, a higher PA (15 $m^3 \cdot h^{-1}$) effectively decreased the EFs of PM ($P < 0.05$) by ~60% to ~80% in the nine sizes. However, when SA was set as 15 $m^3 \cdot h^{-1}$, no significant differences were found in EF_{PM} between the two different PAs ($P > 0.05$). It is also noticed that EF_{PM} was not significantly different between Tests 6 and 8 (both with SA = 15 $m^3 \cdot h^{-1}$) and Test 7 (with SA = 1.5 $m^3 \cdot h^{-1}$, PA = 15 $m^3 \cdot h^{-1}$). Besides, these tests also showed similar PM size distributions pattern. This suggests that EF_{PM} could be maintained at relatively low levels under certain air supply conditions, if PA and SA matched properly.

3.3. Implication of air supply on EFs of carbonaceous species

Fig. 5 shows the mass fractions of OC and EC in $PM_{2.5}$ emitted from different air supply tests. For the total carbon (TC), Test 4 yields the lowest EFs of TC (EF_{TC}) (69.3 mg·MJ^{-1}) among all the tests, > 90% lower than in Test 1 (1061.8 mg·MJ^{-1}). Test 4 had very low OC1 and OC2 fractions, only accounting for about 20% of TC. These two compounds were generally deemed as the products of low temperature combustion or smoldering (Ni et al., 2015). Noticeably, OP (Pyrolyzed OC),which was also attributed to smoldering products in previous studies (Han et al., 2010; Ni et al., 2015), showed a higher proportion in Tests 1, 2, 6 and 8. The high OP proportion in Test 1 was due to deficient air supply while in Tests 6 and 8 due to cooled temperature in combustion chamber because of the high SA. A common phenomenon in all the tests was the high and frequently dominant EC1 content because EC1 was commonly produced in low temperature combustion such as biomass burning (Chow et al., 2007; Han et al., 2010), and combustion in semi-gasification stove could not achieve a high-enough temperature for producing EC2 and EC3.

Size segregated OC and EC are shown in Fig. 6 and Fig. S2. In Fig. 6, results from tests with six varied SA flows are drawn to detect the influence of SA on TC sub-fractions in different PM sizes. Three major findings were found from Fig. 6. The first one was that the highest EF_{TC}

was observed in Test 1 in which SA was set to be very low (0.3 $m^3 \cdot h^{-1}$). It was reported that carbonaceous fractions including OC and EC in combustion productions were mainly due to oxygen deficient (Han et al., 2010). The evidence of oxygen deficient condition in Test 1 (and also Test 2) rather than in other tests was the dramatically high OP in Test 1, an indicator for incomplete combustion. The second finding was that among the eight sub-fractions, OC3 was the highest in OC and EC1 in EC. OC3 was generally deemed as high temperature produced OC, but traditional stoves usually maintain relative low temperatures due to the poor air supply and users' conventions and thus should produce high contents of OC1 and OC2 (Shen et al., 2012; Sun et al., 2017). The third finding was that among the nine measured PM sizes, the finest phase (PM diameter < 0.47 μm) had the most abundant carbon fraction under any air supply condition. $PM_{1.1}$ OC and EC accounted for > 70% and 90%, respectively, of total PM OC and EC. It has been reported that ultra-fine and even smaller particles (PM diameter < 0.47 μm) dominated in PM size distribution from wood combustion (Shen et al., 2010), and it has been proved that these particles were soot-related (Purvis and McCrillis, 2000; Danielsen et al., 2011). However, the production mechanisms of EC and even OC still need further investigation for clarification.

The impact of PA on carbonaceous fractions in size segregated PM was shown in Fig. S2. A higher PA (15 $m^3 \cdot h^{-1}$) emitted much lower carbon sub-fractions than a lower PA (6 $m^3 \cdot h^{-1}$) ($P < 0.05$) in low SA conditions (1.5 $m^3 \cdot h^{-1}$). When PA was set as 6 $m^3 \cdot h^{-1}$, a remarkable amount of EF of OP (EF_{OP}) was emitted in the finest particle size (< 0.47 μm) indicating oxygen deficiency burning condition.

4. Conclusion

The impacts of air supply in wood burning in a semi-gasification stove on size segregated emissions of PM and carbonaceous species were evaluated. The results proved that both primary and secondary air supply have crucial effects on EFs of PM. PA had a linear effect on EFs of PM and carbonaceous species while SA had a quadric effect under conditions set in this study. EFs decreased with PA rising, but increased when SA deviated from 7 $m^3 \cdot h^{-1}$. The lowest EFs of $PM_{2.5}$, OC, and EC were found on the conditions with PA being 6 $m^3 \cdot h^{-1}$ and SA being 7 $m^3 \cdot h^{-1}$. For size segregated PM, EFs of PM were the lowest at SA values of 7 and 10 $m^3 \cdot h^{-1}$ in all the nine size stages. Among the nine measured PM sizes, the finest phase (PM diameter < 0.47 μm) had the highest EFs and also the most abundant carbon fraction under any air supply conditions. More studies are needed to investigate the mechanisms of air supply on size segregated particles emitted from stove burning of other biomass fuels.

Acknowledgements

This research was supported by the Natural Science Foundation of Shaanxi Province, China (2016ZDJC-22), National Natural Science Foundation of China (41573101), National Key Research and Development Plan of China (2017YFC0212205), State Key Laboratory of Loess and Quaternary Geology, Institute of Earth Environment, CAS (SKLLQG1616), the Fundamental Research Funding for Central Universities in China (xkjc2015002), and the Key Lab of Aerosol Chemistry & Physics of the Chinese Academy of Sciences (KLACP201501).

Appendix A. Supplementary data

Supplementary data to this article can be found online at https://doi.org/10.1016/j.atmosres.2017.11.010.

Reference

Bailis, P.R., Ogle, D., Maccarty, N., From, D.S.I., Smith, K.R., Edwards, R., Energy, H., 2007. The Water Boiling Test (WBT).

Bonjour, S., Adair-Rohani, H., Wolf, J., Bruce, N.G., Mehta, S., Pruss-Ustun, A., Lahiff, M., Rehfuess, E.A., Mishra, V., Smith, K.R., 2013. Solid fuel use for household cooking: country and regional estimates for 1980–2010. Environ. Health Perspect. 121 (7), 784–790.

Chen, Y., Roden, C.A., Bond, T.C., 2012. Characterizing biofuel combustion with patterns of real-time emission data (PaRTED). Environ. Sci. Technol. 46 (11), 6110–6117.

Chow, J.C., Watson, J.G., Chen, L.W.A., Chang, M.C.O., Robinson, N.F., Trimble, D., Kohl, S., 2007. The IMPROVE-A temperature protocol for thermal/optical carbon analysis: maintaining consistency with a long-term database. J. Air Waste Manage. Assoc. 57 (9), 1014–1023.

Chowdhury, Z., Campanella, L., Gray, C., Al Masud, A., Marter-Kenyon, J., Pennise, D., Charron, D., Zuzhang, X., 2013. Measurement and modeling of indoor air pollution in rural households with multiple stove interventions in Yunnan, China. Atmos. Environ. 67, 161–169.

Danielsen, P.H., Moller, P., Jensen, K.A., Sharma, A.K., Wallin, H., Bossi, R., Autrup, H., Molhave, L., Ravanat, J.-L., Briede, J.J., de Kok, T.M., Loft, S., 2011. Oxidative stress, DNA damage, and inflammation induced by ambient air and wood smoke particulate matter in human A549 and THP-1 cell lines. Chem. Res. Toxicol. 24 (2), 168–184.

Han, Y.M., Cao, J.J., Lee, S.C., Ho, K.F., An, Z.S., 2010. Different characteristics of char and soot in the atmosphere and their ratio as an indicator for source identification in Xi'an, China. Atmos. Chem. Phys. 10 (2), 595–607.

Hedberg, E., Kristensson, A., Ohlsson, M., Johansson, C., Johansson, P.A., Swietlicki, E., Vesely, V., Wideqvist, U., Westerholm, R., 2002. Chemical and physical characterization of emissions from birch wood combustion in a wood stove. Atmos. Environ. 36 (30), 4823–4837.

Houshfar, E., Skreiberg, O., Lovas, T., Todorovic, D., Sorum, L., 2011. Effect of excess air ratio and temperature on NOx emission from grate combustion of biomass in the staged air combustion scenario. Energy Fuel 25 (10), 4643–4654.

Jetter, J., Zhao, Y.X., Smith, K.R., Khan, B., Yelverton, T., DeCarlo, P., Hays, M.D., 2012. Pollutant emissions and energy efficiency under controlled conditions for household biomass cookstoves and implications for metrics useful in setting international test standards. Environ. Sci. Technol. 46 (19), 10827–10834.

Johansson, L.S., Tullin, C., Leckner, B., Sjovall, P., 2003. Particle emissions from biomass combustion in small combustors. Biomass Bioenergy 25 (4), 435–446.

Kirch, T., Birzer, C.H., Medwell, P.R., Holden, L., 2016. The role of primary and secondary air on wood combustion in cookstoves. Int. J. Sust. Energy 1 (10), 1–10.

Kjallstrand, J., Olsson, M., 2004. Chimney emissions from small-scale burning of pellets and fuelwood - examples referring to different combustion appliances. Biomass Bioenergy 27 (6), 557–561.

Kshirsagar, M.P., Kalamkar, V.R., 2014. A comprehensive review on biomass cookstoves and a systematic approach for modern cookstove design. Renew. Sust. Energ. Rev. 30, 580–603.

Kumar, M., Kumar, S., Tyagi, S.K., 2013. Design, development and technological advancement in the biomass cookstoves: a review. Renew. Sust. Energ. Rev. 26, 265–285.

Lei, Y., Zhang, Q., He, K.B., Streets, D.G., 2011. Primary anthropogenic aerosol emission trends for China, 1990–2005. Atmos. Chem. Phys. 11 (3), 931–954.

Liu, J.Y., Zhai, G.X., Chen, R.Y., 2001. Analysis on the characteristics of biomass fuel direct combustion process. J. Northeast Agric. Univ. 32 (3), 290–294.

MacCarty, N., Still, D., Ogle, D., 2010. Fuel use and emissions performance of fifty cooking stoves in the laboratory and related benchmarks of performance. Energy Sustain. Dev. 14 (3), 161–171.

McMeeking, G.R., Kreidenweis, S.M., Baker, S., Carrico, C.M., Chow, J.C., Collett Jr., J.L., Hao, W.M., Holden, A.S., Kirchstetter, T.W., Malm, W.C., Moosmueller, H., Sullivan, A.P., Wold, C.E., 2009. Emissions of trace gases and aerosols during the open combustion of biomass in the laboratory. J. Geophys. Res. Atmos. 114 (D19).

Ni, H.Y., Han, Y.M., Cao, J.J., Chen, L.W.A., Tian, J., Wang, X.L., Chow, J.C., Watson, J.G., Wang, Q.Y., Wang, P., Li, H., Huang, R.J., 2015. Emission characteristics of carbonaceous particles and trace gases from open burning of crop residues in China. Atmos. Environ. 123, 399–406.

Purvis, C.R., McCrillis, R.C., 2000. Fine particulate matter (PM) and organic speciation of fireplace emissions. Environ. Sci. Technol. 34 (9), 1653–1658.

Raman, P., Ram, N.K., Gupta, R., 2014. Development, design and performance analysis of a forced draft clean combustion cookstove powered by a thermo electric generator with multi-utility options. Energy 69, 813–825.

Ryu, C., Yang, Y.B., Khor, A., Yates, N.E., Sharifi, V.N., Swithenbank, J., 2006. Effect of fuel properties on biomass combustion: part I. Experiments - fuel type, equivalence ratio and particle size. Fuel 85 (7–8), 1039–1046.

Shen, Z.X., Cao, J.J., Arimoto, R., Han, Z.W., Zhang, R.J., Han, Y.M., Liu, S.X., Okuda, T., Nakao, S., Tanaka, S., 2009. Ionic composition of TSP and $PM_{2.5}$ during dust storms and air pollution. Atmos. Environ. 43, 2911–2918.

Shen, G.F., Yang, Y., Wang, W., Tao, S., Zhu, C., Min, Y., Xue, M., Ding, J., Wang, B., Wang, R., Shen, H.Z., Li, W., Wang, X.L., Russell, A.G., 2010. Emission factors of particulate matter and elemental carbon for crop residues and coals burned in typical household stoves in China. Environ. Sci. Technol. 44 (18), 7157–7162.

Shen, G.F., Wei, S.Y., Wei, W., Zhang, Y.Y., Min, Y.J., Wang, B., Wang, R., Li, W., Shen, H.Z., Huang, Y., Yang, Y.F., Wang, W., Wang, X.L., Wang, X.J., Tao, S., 2012. Emission factors, size distributions, and emission inventories of carbonaceous particulate matter from residential wood combustion in rural China. Environ. Sci. Technol. 46 (7), 4207–4214.

Shen, G.F., Xue, M., Wei, S.Y., Chen, Y., Wang, B., Wang, R., Shen, H.Z., Li, W., Zhang, Y.Y., Huang, Y., Chen, H., Wei, W., Zhao, Q., Li, B., Wu, H., Tao, S., 2013. Influence of fuel mass load, oxygen supply and burning rate on emission factor and size distribution of carbonaceous particulate matter from indoor corn straw burning. J. Environ. Sci. 25 (3), 511–519.

Simoneit, B.R.T., 2002. Biomass burning - a review of organic tracers for smoke from incomplete combustion. Appl. Geochem. 17 (3), 129–162.
Sun, J., Shen, Z.X., Cao, J.J., Zhang, L.M., Wu, T.T., Zhang, Q., Yin, X.L., Lei, Y.L., Huang, Y., Huang, R.J., Liu, S.X., Han, Y.M., Xu, H.M., Zheng, C.L., Liu, P.P., 2017. Particulate matters emitted from maize straw burning for winter heating in rural areas in Guanzhong Plain, China: current emission and future reduction. Atmos. Res. 184, 66–76.
Tian, J., Chow, J.C., Cao, J.J., Han, Y.M., Ni, H., Chen, L.W.A., Wang, X., Huang, R., Moosmueller, H., Watson, J.G., 2015. A biomass combustion chamber: design, evaluation, and a case study of wheat straw combustion emission tests. Aerosol Air Qual. Res. 15 (5), 2104–2114.
Wang, X., Chancellor, G., Evenstad, J., Farnsworth, J.E., Hase, A., Olson, G.M., Sreenath, A., Agarwal, J.K., 2009. A novel optical instrument for estimating size segregated aerosol mass concentration in real time. Aerosol Sci. Technol. 43 (9), 939–950.
Wang, R., Tao, S., Wang, W., Liu, J., Shen, H., Shen, G., Wang, B., Liu, X., Li, W., Huang, Y., Zhang, Y., Lu, Y., Chen, H., Chen, Y., Wang, C., Zhu, D., Wang, X., Li, B., Liu, W., Ma, J., 2012. Black carbon emissions in China from 1949 to 2050. Environ. Sci. Technol. 46 (14), 7595–7603.
WHO, 2014. Household Air Pollution and Health – Fact Sheet N 292.
Wiinikka, H., Gebart, R., 2005. The influence of air distribution rate on particle emissions in fixed bed combustion of biomass. Combust. Sci. Technol. 177 (9), 1747–1766.
Xie, J.J., Yang, X.M., Zhang, L., Ding, T.L., Song, W.L., Lin, W.G., 2007. Emissions of SO_2, NO and N_2O in a circulating fluidized bed combustor during co-firing coal and biomass. J. Environ. Sci. 19 (1), 109–116.
Xu, S.S.L., W.X., Tao, S., 2006. Emission of polycyclic aromatic hydrocarbons in China. Environ. Sci. Technol. 40 (3), 702–708.
Xu, Y., Wang, Y., Chen, Y.J., Tian, C.G., Feng, Y.L., Li, J., Zhang, G., 2016. Characterization of fine and carbonaceous particles emissions from pelletized biomass-coal blends combustion: implications on residential crop residue utilization in China. Atmos. Environ. 141, 312–319.